Research Article

In-silico investigation of oxoaporphine alkaloids of *Xylopia aethiopica* against SARS-COV-2 main protease

Babatunde Temitope Ogunyemi[1] and Ogunyemi Olajide Oderinlo[2]*

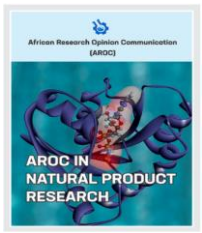

[1]Physical and Computational Chemistry Unit, Department of Chemistry, Federal University Otuoke, Bayelsa State
[2]Natural Product Drug Discovery Group, Department of Chemistry, Federal University Otuoke, Bayelsa State

Corresponding author* Ogunyemi Olajide Oderinlo; oderinlooo@fuotuoke.edu.ng
Received: 18 January 2022, Revised: 15 February 2022, Published: 25 February 2022
https://doi.org/10.53858/arocnpr02010112

Abstract

Background: The ongoing coronavirus pandemic poses a significant social, economic, and health threat worldwide. The situation is exacerbated further by vaccine hesitancy and the ongoing development of mutant strains that could lead to drug resistance. It is therefore critical to find new anti-viral chemotherapeutic agents to reduce or end the epidemic. This study aimed to investigate the antiprotease activity of the oxoaporphine alkaloids in *Xylopia aethiopica*. **Methods:** Computational techniques such as molecular docking were used to probe the oxoaporphine alkaloids in the plant for their ability to inhibit the main protease of Severe Acute Respiratory Syndrome Coronavirus-2 (SARS-CoV-2). The docking score calculations which quantifies the predictive binding affinity of both ligand and target was carried out using Auto-Dock Vina software. **Results:** The results showed that oxoaporphine alkaloids had a better binding affinity than hydroxychloroquine sulfate (standard). Similarly, the values of the chemical descriptors obtained for these alkaloids revealed notable profiles, and these alkaloids also have good oral bioavailability according to rule of five. **Conclusion:** These findings imply that these plant-based alkaloids could be investigated further as prospective leads against SARS-CoV-2 main protease. Furthermore, structural-activity relationships on these compounds could be an effective way to mitigate the predicted side effects.

Keyword: COVID-19; *Xylopia aethiopica*; oxoaporphine alkaloid; molecular docking; Main protease;

Citations: Ogunyemi, B.T., and Oderinlo, O.O. (2022). In-silico investigation of oxoaporphine alkaloids of *Xylopia aethiopica* against SARS-COV-2 main protease. AROC in Natural Products Research, 2(1);01-12, https://doi.org/10.53858/arocnpr02010112

1.0 Introduction

The 2019 coronavirus disease also referred to as COVID-19 is caused by a new coronavirus termed Severe Acute Respiratory Syndrome Coronavirus-2 (SARS-CoV-2), which broke out in Wuhan city in December 2019 [1]. SARS-CoV-2 is the seventh member of the *β*-coronavirus family that afflict humans [2], and it is seemly more contagious and infectious than its close relatives, Middle East respiratory syndrome (MERS) and severe acute respiratory syndrome (SARS) [3]. SARS-CoV-2 is highly pathogenic, primarily targeting the human respiratory system thereby causing severe symptoms or even death [4, 5].

The virus has so far infected more than 400 million people with a death toll of over 5.7 million [6]. Considering the significant mortality and morbidity, as well as the social and economic burden posed by COVID-19 worldwide, it is therefore critical to continue the search for target specific chemotherapeutical agents to treat this viral disease. The main protease (M^{pro}) of SARS-CoV-2 plays a pivotal role in viral replication and transcription [7], and also in virus entry to host cells [5]. These functional properties of M^{pro}, coupled with the fact that no closely related homologues in human [7], makes it an attractive target for anti-viral drug development.

Plants are reservoirs of many bioactive molecules which have been traditionally explored in treating various human and animal diseases [8, 9]. Phytochemicals in plants such as flavonoids, polyphenols, terpenoids and alkaloids, play a crucial role in the drug discovery and development process [10]. Alkaloids in particular have been documented to possess a wide range of pharmacological activities, including antiviral, antioxidant, anti-inflammatory, antineoplastic and immunomodulatory properties [11, 12]. We recently profiled some herbal plants used in COVID-19 management in Southwestern Nigeria, which include *Xylopia aethiopica* (*X. aethiopica*) [13].

X. aethiopica, also known as Negro pepper, is an aromatic, evergreen tree native to the African Savanna region, specifically Ethiopia, Senegal, Ghana, Nigeria, and Cameroon [14]. The seed is widely used as a spice and in traditional medicine. It is a treasure trove of biological activities; it has been reported to

possess anticancer, antidiabetic, antimalarial, analgesic, antioxidant, enzyme inhibitory, antimicrobial, and antibacterial and antiviral properties [14-16].

While isolation and characterization are critical steps in the identification of bioactive molecules in natural product drug discovery, computational techniques such as molecular docking, density functional theory (DFT), physiologically-based pharmacokinetic modelling, and others are becoming increasingly more popular for identifying of likely bioactive secondary metabolites in a timely and efficient manner [17]. For instance, the most widely used approach, DFT, has a lower computational cost than many other methods and is used to predict various properties of organic molecules including bond length, bond angles, dihedral angles and toxicity amongst others [18-20]. Molecular docking is commonly used to determine the appropriate orientation of molecules in the active site of the receptors of interest, and as well as determine their binding affinity. In essence, it is used to investigate the biological activity of molecules [21, 22].

Similarly, physiological-based drug metabolism and pharmacokinetic (DMPK) modelling that predict absorption, distribution, metabolism, excretion and the potential for toxicity (ADMET) in humans are critical to the success of any molecule. It is critical to implement some DMPK/ADMET-based limits early on in the discovery process in order to reduce the number of compounds required for evaluation and save time and resources [23]. Therefore, the bioactive compounds that can be isolated experimentally from medicinal plants can also be theoretically studied using these computational tools. Hence, given the rapid global spread of the coronavirus and the continual development of mutant strains that could lead to drug resistance, finding new anti-viral agents to reduce or end the epidemic health implications is critical. The primary objective is to evaluate potent pharmacological properties and the antiviral activity of presented oxoaporphine alkaloids against SARS-COV-2 main protease.

2.0 Methodology

2.1 Ligands and receptor selection

In this study, the oxoaporphine alkaloids previously identified in *X. aethiopica* were used [24]. These alkaloids were used as ligands against the M^{pro} target protein of SARS-CoV-2 retrieved from the protein data bank (https://www.rcsb.org/structure/6LU7). This three-dimensional crystal structure SARS-CoV-2 (PBD IDs: 6LU7) was selected because it was recently released, highly conserved in nature with high resolution (1.8 Å) and recognized by the X-ray diffraction technique. The three-dimensional structure of M^{pro} and its interactive co-crystallized ligand site on its structure is represented in Figure 1a.

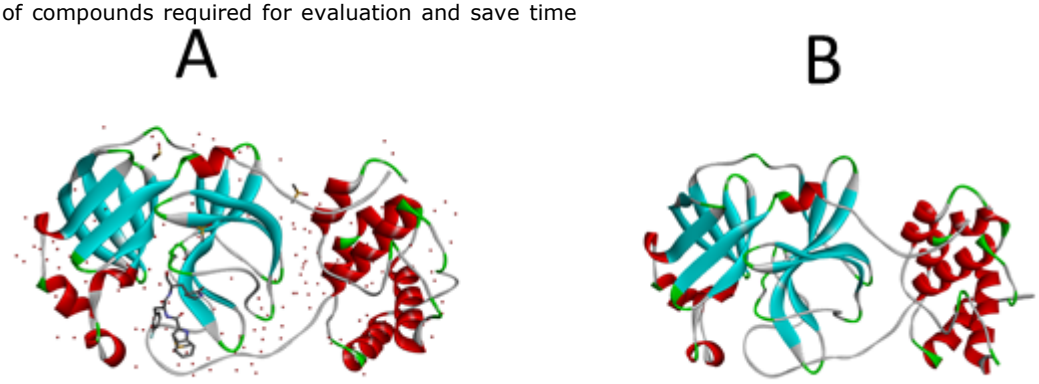

Figure 1: (a) M^{pro} and its interactive co-crystallized ligand site on its structure (b) The crystal structure of prepared M^{pro} without crystallized inhibitor N3 and water molecules

2.2 Receptor and ligands preparation

With the aid of discovery studio software, the inhibitor and water molecules were removed from the target protein (Figure 1b). This treated target protein was imported into Auto dock 4.2, where hydrogen atoms were added to the protein to correct the ionization and tautomeric states of the amino acid residues. Further, Kollman charges were added [25]. The dimensions of the grid box and receptor setup were x= 50 Å, y= 54 Å, z = 48 Å and x = -26.401 Å, y = 13.54 Å, z =40 Å during docking study, respectively, with a grid space of 1 Å. The accurate and reliable three-dimensional structure of the target protein was investigated using PROCHECK server which creates a Ramachandran plot, which shows the allowed and disallowed areas regarding backbone dihedrals of protein residues. Furthermore, the selected bioactive alkaloids from *X. aethiopica* (Figure 2, Table 1) were optimized using Spartan software. Optimized molecules were then saved in pdb format for molecular docking with the SARS-CoV-2 M^{pro}.

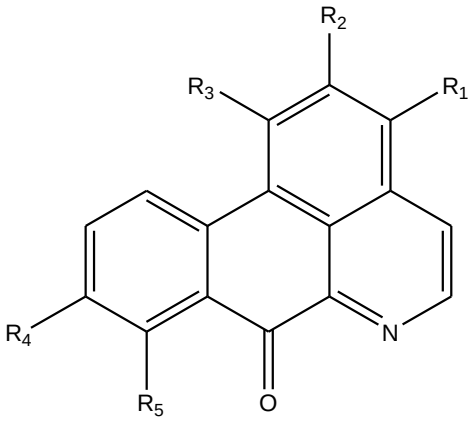

Figure 2: Structural backbone of the selected oxoaporphine alkaloids from *X. aethiopica*

2.3 Pharmacokinetic study

The preADMET server (Korea) (https://preadmet.webservice.bmdrc.org/) and admetSAR server (http://lmmd.ecust.edu.cn/admetsar1) were used to predict the ADMET of all the studied alkaloids [26]. In this study, several parameters such as human intestinal absorption, Ames test blood-brain barrier, Caco-2 cell permeability, human Ether-à-go-go-Related Gene, carcinogenicity, molecular weight, hydrogen bond acceptor, hydrogen bond donor, topological polar surface area were considered.

Table 1: Substituent pattern on the oxoaporphine alkaloids in figure 2

Alkaloid	**representation**	**R_1**	**R_2**	**R_3**	**R_4**	**R_5**
Liriodenine	Ligand 1	H	O-CH_2-	-O-	H	H
Lysicamine	Ligand 2	H	O-CH_3	O-CH_3	H	H
o-Methylmoschatoline	Ligand 3	O-CH_3	O-CH_3	O-CH_3	H	H
Oxoglaucine	Ligand 4	H	O-CH_3	O-CH_3	O-CH_3	O-CH_3
Oxophoebine	Ligand 5	O-CH_3	O-CH_3	O-CH_3	O-CH_2	-O

2.4 Molecular docking of ligand-protein

To predict the binding affinity and activity of the ligand molecule, molecular docking is utilized to determine the scoring function and assess protein-ligand interactions [27]. The bioactive binding poses of the ligands dataset in the active site of SARS-CoV-2 M^{pro} were generated using the Auto dock tool. As a result, the scoring function was generated using the Lamarckian genetic algorithm's usual technique [25]. During docking, target protein was centered on the grid map. The hydrophobic and non-bonded polar interactions at the inhibitor site of 6LU7 were modeled using Accelrys Discovery Studio 2019 software (Biovia, 2017). Discovery Studio Visualizer 4.0 was used to visualize the docking findings.

3.0 Results and discussion

3.1. Grid generation and protein structural reliability

The precise and dependable three-dimensional structure of the target protein is required for drug development. Figures 3 A and B shows that 91.2 percent of the residues in the target protein's three-dimensional structure are in the most preferred area, while just 0.6 percent are in the prohibited zone (PDB ID: 6LU7). The requirement for becoming a model of excellent quality is to have more than 90% of residues in preferred areas.

3.2. Quantum Chemical Calculations.

Molecular chemical descriptors: highest occupied molecular orbital energy (E_{HOMO}), lowest unoccupied molecular orbital energy (E_{LUMO}), energy bandgap, log P, polarizability, dipole moment (DM), area volume, hydrogen bond donor, polar surface area and hydrogen bond acceptor (Table 3) were calculated for all the studied alkaloids via DFT with Becke three parameter exchange and Lee−Yang−Parr correlation (B3LYP) and 6-31+G(d,p) basis sets. The E_{HOMO}, E_{LUMO} and band gap energies provide qualitative information on the excitation characteristics and enzyme binding of modeled complex [28, 29] which in turn determines the extent of non-bonding interactions such as hydrophilic interactions and hydrogen bonding between the ligand and the receptor. The estimated E_{HOMO} values, which reflect the potential of drug-like molecules to donate electrons to the nearby molecules, were −6.03 eV (liriodenine), −5.72 eV (lysicamine), −5.37 eV (o-methylmoschatoline), −5.54 eV (oxophoebine), and −5.24 eV (oxoglaucine). As shown in Table 3, oxoglaucine is expected to donate more electrons than the other

oxoaporphine alkaloids investigated. The E_{LUMO} demonstrate the compounds capability to accept electrons from neighboring molecules. Thus, the Liriodenine which has E_{LUMO} of −2.40 eV, is predicted to have a better capability to accept electron from the neighboring molecule than other oxoaporphine alkaloids investigated. Band gap is an important parameter that indicates the extent of ligand-protein interaction between the bioactive compounds and the protein(s) under study. The lower the band gap, the better a compound's ability to donate electrons to the neighbouring molecules. The order of the band gap is oxoglaucine < oxophoebine < o-methylmoschatoline < lysicamine < liriodenine (Table 3). Therefore, oxoglaucine is expected to react better than other studied compounds. The analysis of frontier molecule orbital density distributions of the compounds under study: HOMO (right), LUMO (left) (Table 4) shows that their electron density distribution on HOMO and LUMO are localized in the atoms of the aromatic cycles of the five compounds.

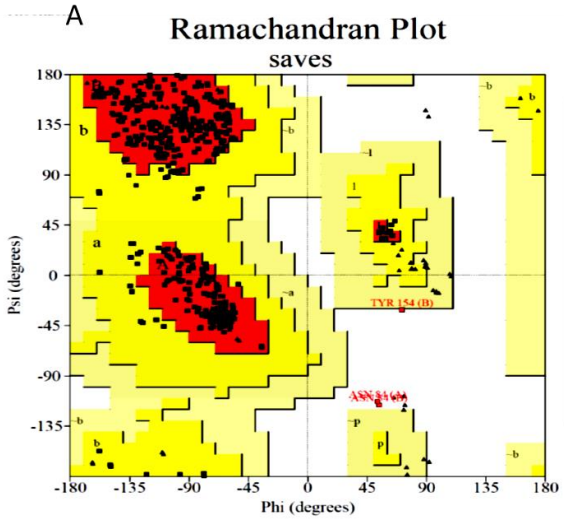

B

Residues in most favored regions [A, B, L]	476	91.2%
Residues in additional allowed regions	43	8.2%
Residues in generously allowed region	0	0.0%
Residues in disallowed regions	3	0.6%
Number of non-glycine and non-proline residue	522	100%
Number of end-residues (excl, Gly and Pro)	4	
Number of glycine residues (shown as triangles)	50	
Number of proline residues	26	
Total number of residues	602	

Figure 3: Grid generation and protein structural reliability. (A) Ramachandran plot showing the reliability of the target protein. (B) Statistical analysis of the Ramachandran Plot. Based on the analysis of 118 structures of resolution of at least 2.0 Angstroms and R-factor no greater than 20%, a quality model would be expected to have over 90% in the most favoured regions.

Table 3: Calculated molecular descriptors of the studied compounds

Alkaloids	E_{HOMO}	E_{LUMO}	BG	Log P	MW	DM	POL	HBD	HBA	OVA	PSA
Liriodenine	-6.03	-2.40	3.63	0.04	275.3	6.95	61.61	0	4	1.32	35.43
Lysicamine	-5.72	-2.25	3.47	0.01	291.3	9.17	64.00	0	4	1.38	28.51
o-Methylmoschatoline	-5.37	-2.13	3.24	-0.97	321.3	9.38	66.25	0	5	1.42	30.51
Oxoglaucine	-5.24	-2.09	3.15	-0.95	351.4	10.68	68.49	0	6	1.48	39.84
Oxophoebine	-5.54	-2.35	3.19	-2.89	365.3	7.36	68.38	0	7	1.47	53.57

Notes: BG: band gap (E_{LUMO}-E_{HOMO}); DM: dipole moment; MW: molecular weight; OVA: ovality; POL: polarizability; HBD: hydrogen bond donor; HBA: hydrogen bond acceptor.

Table 4: Distribution of frontier molecule orbital density of studied compounds: HOMO (left), LUMO (right).

Alkaloids	HOMO	LUMO
Liriodenine	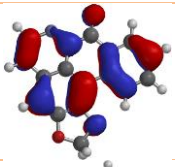	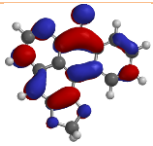
Lysicamine	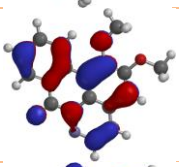	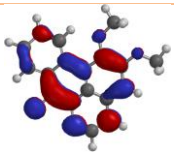
o-Methylmoschatoline	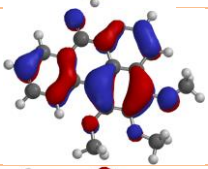	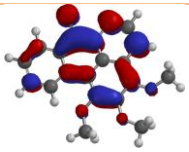
Oxoglaucine	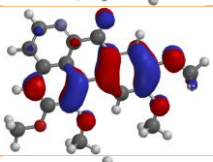	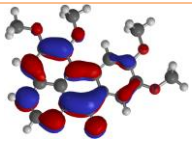
Oxophoebine	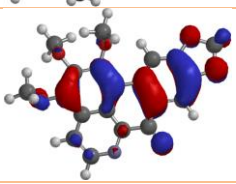	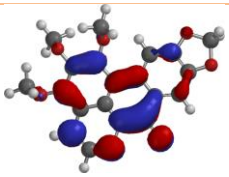

Lipophilicity is one of the essential physicochemical parameters for predicting the 'drugability' of molecules [30]. Lipophilicity refers to the ability of a molecule to partition into the lipid phase or biological membranes, and it can be measured or predicted experimentally by quantifying the distribution of a molecule between the aqueous and nonpolar phases [31, 32]. Lipophilicity, as the foremost drug-like parameter, has a significant impact on solubility, permeability, potency, selectivity, and other drug properties [32, 33]. Lipophilicity is commonly assessed using a calculated log P [34]. If the estimated log P is higher than the usual value for log P (log P ≤ 5), oral absorption, permeability and metabolic stability may be compromised, and the risk of promiscuity against metabolic enzymes and other hydrophobic targets other than the desired targets increases. When compared to Meanwell's log P value [35], the calculated log P values (Table 3) are less than 5, indicating that the five oxoaporphine alkaloids were lipophilicity effective.

The dipole moment of a molecules is the product of the charge at both ends of the dipole of the molecule and the distance between the charges of molecules. The contribution of dipole moment to the biological activity of studied compounds is important. The presence of dipole moment as a non-bonded interaction in the drug-like compound-protein complex affect the relationship between ligand and the enzyme [36]. Furthermore, every single molecule investigated with higher DM value has been reported to have unique properties [37]. The DM of molecular compounds has been determined to range between 3 and 5 kJ/mol [38]. Practically, all of the DM values observed in this investigation are higher than the approved range.

3.3 Energetics and ligand-protein interactions

Docking studies were conducted to observe the interactions between the receptor and the ligand in order to determine the conformation of the molecules in the receptor gouge. It is also used to predict ligand-protein affinity [39]. Table 4 shows the binding affinity (kcal/mol) and interactions of various studied ligands orientations in the active site of the SARS-CoV-2 M^{pro}. Also, Figure 4 a-e, show the pictorial view of the docking simulations performed on the five oxoaporphine alkaloids.

The binding energies of the five alkaloids against the M^{pro} of SARS-CoV-2 vary from −7.0 to −7.9 kcal/mol, demonstrating that all the ligands had similar binding

energies. However, the H-bond length between amino acids and the ligands spans from 1.88 to 3.68 kcal/mol (Table 5). It should be noted that the best ligand (a lead molecule) against COVID-19 is the molecule that binds to the SARS-CoV-2 M^{pro} with a desired effect. It is a compound with the highest binding energy expressed in terms of Gibbs free energy variation (ΔG) from thermodynamic standpoint [40, 41]. Apart from hydrogen bonding, which is the most powerful non-covalent contact for stabilizing complexes, there are a number of other non-covalent interactions that play a role [42], the five ligands show some similarities in interactions involving their aromatic rings. The presence of at least three aromatic rings in both compounds offers many possibilities for π-alkyl and π- π-stacking interactions to take place.

Table 5: Scoring of oxoaporphine alkaloids in *X. aethiopica* with SARS-CoV-2 M^{pro} (PDB ID: 6LU7)

Oxoaporphine Alkaloids	Scoring (kcal/mol)	K_i (μM)	Residues involved in interactions	Distance of H-bond between Amino Acid and ligand (Ă)	Types of Non-bonding interaction involved
Liriodenine	-7.9	5.26 x 10^5	HIS-41, CYS-44, MET-49, MET-165	2.71077, 3.66304	Conventional hydrogen bond, Carbon hydrogen bond, Pi-Cation, Pi-Sulfur, Pi-Alkyl
Lysicamine	-7.0	1.36 x 10^5	GLU-166, CYS-145, MET-165, MET-49	2.16659, 3.61205	Conventional hydrogen bond, Carbon hydrogen bond, Pi-Sulfur Pi-Alkyl, Van de Waals
o-Methylmoschatoline	-7.0	1.36 x 10^5	GLU-166, MET-49, CYS-44, CYS-145, HIS-41,	3.48367, 3.43666	Conventional hydrogen bond, Carbon hydrogen bond, Pi-Sulfur, Pi-Alkyl
Oxoglaucine	-7.5	3.17 x 10^5	GLU-166, MET-165, MET-49, LUE-141, CYS-145	2.17431, 3.59541	Conventional hydrogen bond, Carbon hydrogen bond, Pi-Sulfur, Pi-Alkyl
Oxophoebine	-7.6	3.75 x 10^5	PHE-294, ASP-295, THR-111,	1.8817, 3.68401	Carbon hydrogen bond, Pi-Anion, Pi-Pi Stacked, Van de Waals
Hydroxychloroquine sulfate	-6.1	2.97 x 10^4			

Structurally, liriodenine (ligand 1) formed one H-bond with GLU-166, one carbon hydrogen bond interaction with MET-49, π-alkyl interaction with CYS-145 and eight Van der Waals (vdW) interactions with HIS-41, CYS-44, TYR-54, PRO-52, ASP-187, GLN-189, GLN-192 and ARG-188.

Lysicamine (ligand 2) is characterized by one conventional H-bonding interaction with GLU-166, one carbon hydrogen bond interaction with MET-49, four π-alkyl interaction: three with MET-165 and one with CYS-145, one π-sulphur with MET-165, eight vdW with HIS-41, CYS-44, TYR-54, MET-49, PRO-52, ASP-187, ARG-188, GLN-189 and GLN-192.

o-Methylmoschatoline (ligand 3) is characterized by zero conventional H-bonding interaction, two carbon hydrogen bond interaction with THR-111, four π- π stacked with PHE-294, one π-anion with ASP-295, seven vdW with ASP-153, PHE-8, ASN151, THR-292, GLN-110 PRO-293 and ILE-249

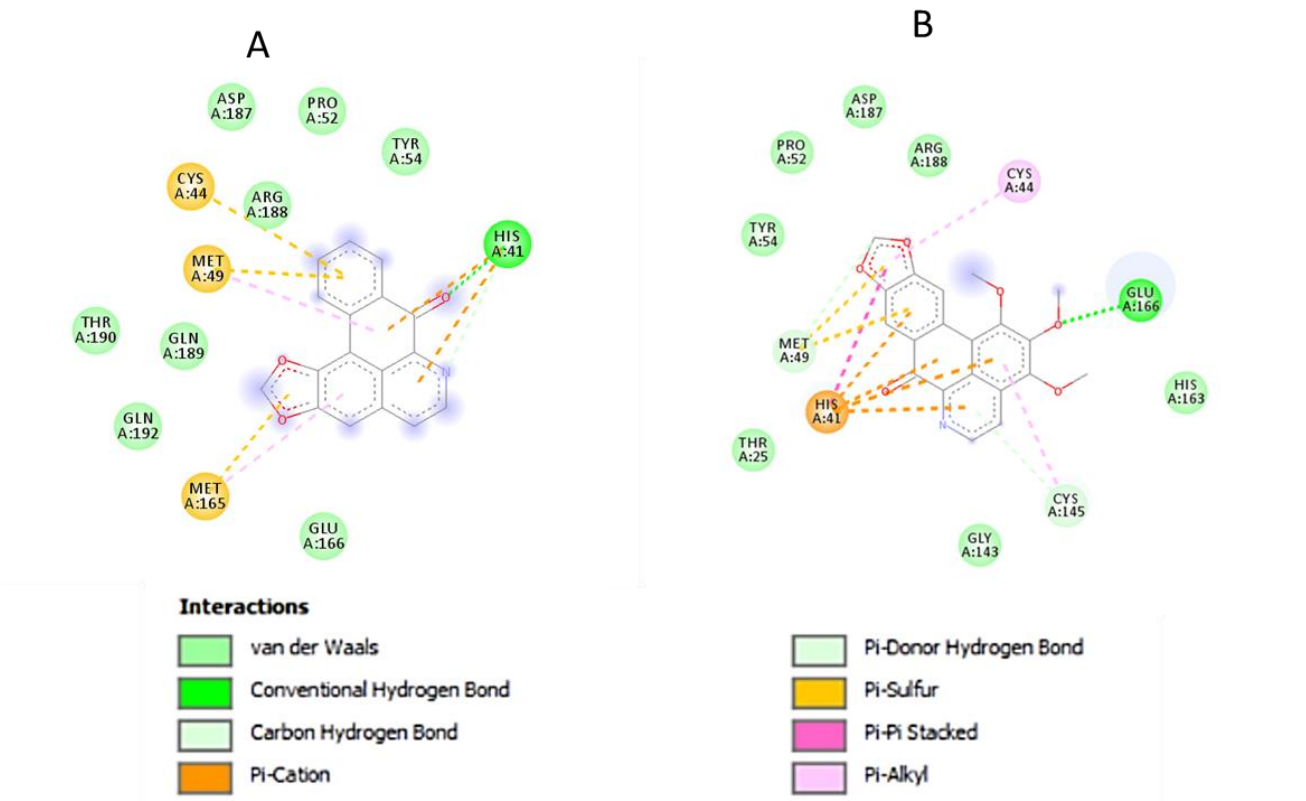

Figure 4a-b: Ligand-receptor interactions in the binding pockets of representative oxoaporphine alkaloids against SARS-CoV-2 M^{pro} (PBD IDs: 6LU7) using discovery studio; (**a**) liriodenine (**b**) oxophoebine.

Oxoglaucine (ligand 4) stabilized its binding with the M^{pro} *via* one conventional H-bonding interaction with GLU-166, two carbon hydrogen bond interaction with MET-49 and LEU-141, four π- alkyl interaction with MET-165 and CYS-145, one π-sulphur with met 165, twelve vdW with GLY-143, ASN-142, SER-144, THR-25, HIS-41, CYS-44, TYR-54, PRO-52, ARG-188, ASP-187, GLN-189 AND GLN-192 (Figure 4)

Oxophoebine (ligand 5) is characterized by one conventional H-bonding interaction with GLU-166, one carbon hydrogen bond interaction with MET-49, four π-cation interaction with HIS-41, four π-alkyl interaction: two with MET-49, one with CYS-44 and one with CYS-145. Two π-sulphur with MET-49, five 165, twelve π- π stacked with HIS-41, π-donor hydrogen bond; Sulphur with CYS-145, ten vdW with GLN- 189, ARG-188, ASP-187, PRO-52, TYR-54, THR-25, GLY-143, ASN-142, HIS-163 and MET-165.

3.4. Prediction of physicochemical properties, drug likeness, pharmacokinetics and toxicity

An important parameter to consider during drug design is the physicochemical property of the molecules under consideration. The oral bioavailability of bioactive compounds were calculated through Lipinski's rule of five and Veber's rule [43], while the Muegge's rule determined the possibility of a compound to become a successful drug molecule by the pharmacophore point calculation [44]. In Lipinski's rule of five: molecular mass < 500; Hydrogen-bond donors (HBD) < 5; Hydrogen-bond acceptors (HBA) < 10; and Log P < 5 [45]. All the compounds adhered to the Lipinski's, Veber's and Muegge's rule, and their values are shown in Table 6. Therefore, the five compounds were predicted to have good bioavailability and satisfied the drug likeliness parameters according to these rules. Consequently, the five oxoaporphine alkaloids may emerge as potential lead for SARS-CoV-2 M^{pro}.

The topological polar surface area (TPSA) gives the surface area containing polar atoms in a compound. When the TPSA is increased, a diminished membrane permeability is observed and compounds with higher TPSA were better substrates for p-glycoprotein, while ligands with lower TPSA value are better in penetrating to the central nervous system [46, 47]. Thus comparing the compounds TPSA, liriodenine, lysicamine and o-methylmoschatoline may be favorable than oxogluacine and oxopoebine (Table 6).

Table 6: Physiochemical properties and drug likeness of the five inhibitors

	Physiochemical properties						Drug likeness			Lipophilicity
Ligands	MW	HBA	HBD	MR	TPSA	NRB	Lipinski violations	Veber violations	Muegge violations	MLog P
1	275.26	4	0	76.7	48.42	0	0	0	0	1.71
2	291.3	4	0	83.6	48.42	2	0	0	0	1.54
3	321.33	5	0	90.1	57.65	3	0	0	0	1.21
4	351.35	6	0	96.6	66.88	4	0	0	0	0.9
5	365.34	7	0	96.2	76.11	3	0	0	0	0.77

MW=molecular weight, HBA=hydrogen bond acceptor, HBD= hydrogen bond donor, MR = molar refractivity, TPSA= topological polar surface area, NRB = number of rotatable bond.

Table 7: Pharmacokinetics and toxicity properties of the five inhibitors

	Pharmacokinetic				Toxicity			
Ligands	**GI absorption**	**HIA**	**CYP450 IP**	**BBB permeant**	**ESOL Class**	**Ames-test**	**Carcino-Rat/mouse**	**hERG**
1	High	0	positive	Yes	Soluble	Mutagen	+/-	Medium risk
2	High	0	positive	Yes	Moderately soluble	Mutagen	+/-	Medium risk
3	High	0	positive	Yes	Moderately soluble	Mutagen	+/-	Medium risk
4	High	0	positive	Yes	Moderately soluble	Mutagen	+/-	Medium risk
5	High	0	positive	Yes	Moderately soluble	Mutagen	+/-	Medium risk

GI = Gastrointestinal, HIA= Human Intestinal Absorption (HIA), IP = Inhibitory Promiscuity, BBB = Blood-Brain Barrier, hERG= human Ether-à-go-go-Related Gene, Carcino-= carcinogenicity.

The results of the pharmacokinetics and toxicity properties of the five oxoaporphine alkaloids are shown in Table 7. All the five compounds show high human intestinal absorption. ADMET properties, as derived from admetSAR server, reveal that the five studied compounds had better Human Intestinal Absorption (HIA) value than the hydroxychloroquine sulfate.

Figure 5b shows that ligands lysicamine, o-methylmoschatoline and oxoglaucine absorbed better than liriodenine and oxophoebine. Greater HIA denotes that the compound could be better absorbed from the intestinal tract upon oral administration. In the case of the hERG inhibition, all the ligands presented a medium risk with ligands 4 and 5 having low end point values of 0.5121 and 0.4838, respectively (Figure 5d).

Moreover, the rodent carcinogenicity in rat and mouse predicted by the preADMET server reveals that all are carcinogenic to rat and non-carcinogenic to mouse. The Ames test that assesses mutagenicity of a compound reveals that the five compounds are mutagenic. The probability of these mutagenicity (as depicted in figure 5c) shows that liriodenine and lysicamine have higher endpoint values. The blood brain barrier (BBB) which selectively regulates the permeability of drugs to the brain shows that the penetration through the Blood-Brain Barrier (BBB) came out to be best for molecule liriodenine and oxophoebine but was not significantly higher than the hydroxychloroquine sulfate molecule (Figure 5a).

CYP450 inhibitory promiscuity property which is refers to the capacity for a drug or chemical to bind to and decrease or diminish the activity of multiple different CYP450 isoform enzymes. CYP450 inhibitory promiscuity values for all studied molecules are positive while that of hydroxychloroquine sulfate is negative.

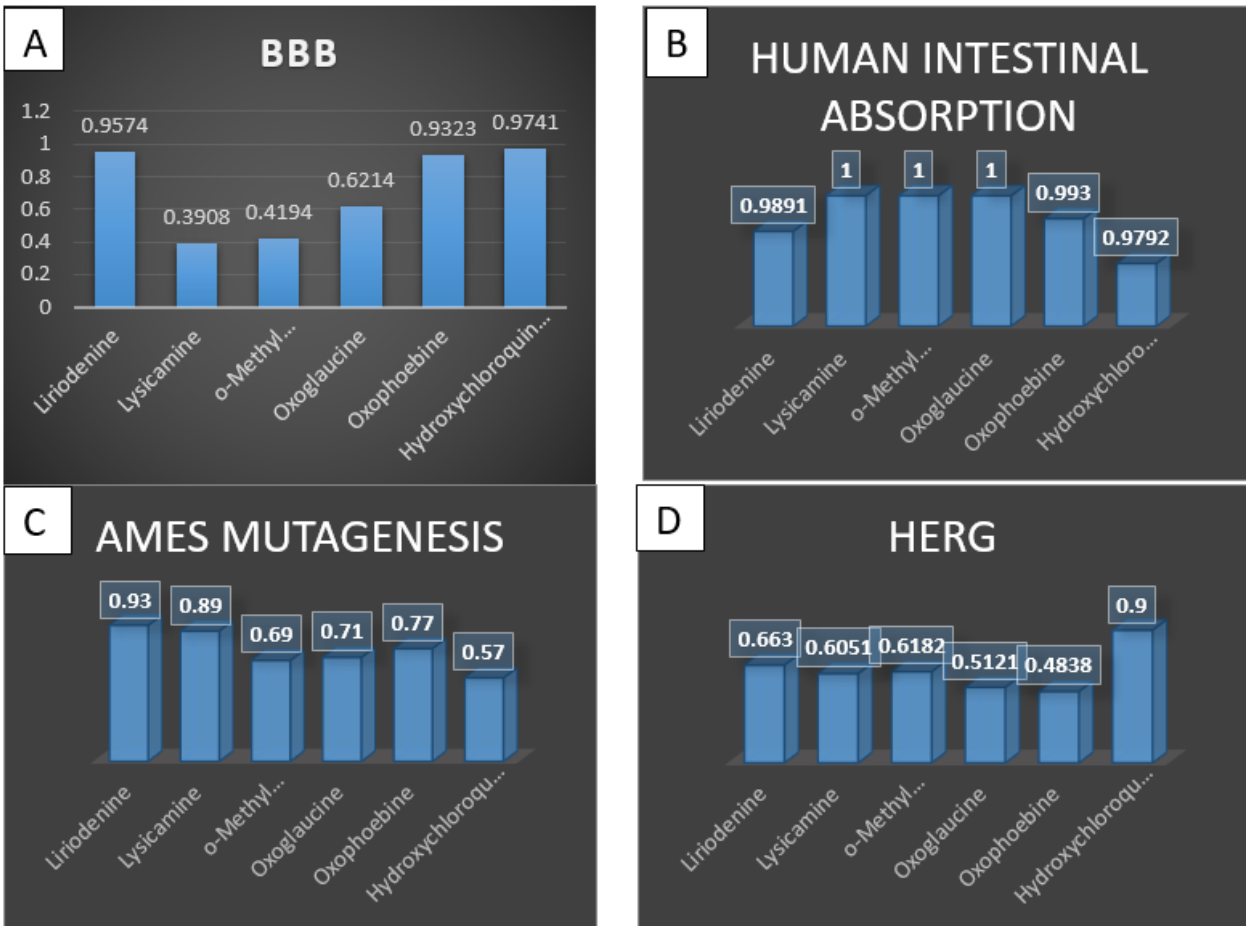

Figure 5: Probability of endpoint values: (a) blood brain barrier (BBB) (b) human intestinal absorption (HIA) (c) Amen mutagenesis (d) human Ether-à-go-go-Related Gene (hERG).

4.0 Conclusion

In this study, quantum chemical method through DFT and docking methods were employed to verify the anti-protease activity of the oxoaporphine alkaloids of *X. aethiopica*. The docking study predicted steady conformations of the ligands in the active site of the enzyme and revealed that natural alkaloids: liriodenine, lysicamine, o-methylmoschatoline, oxoglaucine and oxophoebine had better binding free energies with M^{pro} of SARS-CoV-2 than hydroxychloroquine sulfate. The binding energy value for liriodenine indicates that it has a greater ability to inhibit SARS-CoV-2 M^{pro} than other alkaloids studied, which is further supported by the inhibition constant. Although toxicity properties of liriodenine, lysicamine, o-methylmoschatoline, oxoglaucine and oxophoebine are mutagenic, they have good oral availability and also meet RO5 criteria. Notwithstanding, there are literature evidences that structural modifications can mitigate their potential carcinogenic/mutagenic effects. These results are only preliminary screening to facilitate subsequent *in vitro* and *in vivo* investigations, and further structural-activity relationship in order to mitigate the predicted side effects.

Author contributions: OBT and OOO designed the project, OBT performed the *in silico* experiment. Both authors analysed the data and prepared the manuscript.

Conflict of interest: The authors declare no conflict of interest.

Funding: The authors did not receive any fund for the execution of this project.

References

1. Zhu, H.; Wei, L.; Niu, P., The novel coronavirus outbreak in Wuhan, China. *Global Health Research and Policy* **2020,** 5, (1), 6.

2. Wu, D.; Wu, T.; Liu, Q.; Yang, Z., The SARS-CoV-2 outbreak: What we know. *International Journal of Infectious Diseases* **2020,** 94, 44-48.

3. Zhang, Y.-y.; Li, B.-r.; Ning, B.-t., The Comparative Immunological Characteristics of SARS-CoV, MERS-CoV, and SARS-CoV-2 Coronavirus Infections. *Frontiers in Immunology* **2020,** 11.

4. Ye, Z.-W.; Yuan, S.; Yuen, K.-S.; Fung, S.-Y.; Chan, C.-P.; Jin, D.-Y., Zoonotic origins of human coronaviruses. *International journal of biological sciences* **2020,** 16, (10), 1686-1697.

5. Mengist, H. M.; Dilnessa, T.; Jin, T., Structural Basis of Potential Inhibitors Targeting SARS-CoV-2 Main Protease. *Frontiers in Chemistry* **2021,** 9.

6. WHO World Health Organization Coronavirus (COVID-19) Dashboard. https://covid19.who.int/ (14-02-2022),

7. Jin, Z.; Du, X.; Xu, Y.; Deng, Y.; Liu, M.; Zhao, Y.; Zhang, B.; Li, X.; Zhang, L.; Peng, C.; Duan, Y.; Yu, J.; Wang, L.; Yang, K.; Liu, F.; Jiang, R.; Yang, X.; You, T.; Liu, X.; Yang, X.; Bai, F.; Liu, H.; Liu, X.; Guddat, L. W.; Xu, W.; Xiao, G.; Qin, C.; Shi, Z.; Jiang, H.; Rao, Z.; Yang, H., Structure of Mpro from SARS-CoV-2 and discovery of its inhibitors. *Nature* **2020,** 582, (7811), 289-293.

8. Anand, U.; Jacobo-Herrera, N.; Altemimi, A.; Lakhssassi, N., A Comprehensive Review on Medicinal Plants as Antimicrobial Therapeutics: Potential Avenues of Biocompatible Drug Discovery. *Metabolites* **2019,** 9, (11), 258.

9. Mushtaq, S.; Abbasi, B. H.; Uzair, B.; Abbasi, R., Natural products as reservoirs of novel therapeutic agents. *EXCLI journal* **2018,** 17, 420-451.

10. Mgbeahuruike, E. E.; Yrjönen, T.; Vuorela, H.; Holm, Y., Bioactive compounds from medicinal plants: Focus on Piper species. *South African Journal of Botany* **2017,** 112, 54-69.

11. Ghildiyal, R.; Prakash, V.; Chaudhary, V. K.; Gupta, V.; Gabrani, R., Phytochemicals as Antiviral Agents: Recent Updates. In *Plant-derived Bioactives: Production, Properties and Therapeutic Applications*, Swamy, M. K., Ed. Springer Singapore: Singapore, 2020; pp 279-295.

12. Ti, H.; Zhuang, Z.; Yu, Q.; Wang, S., Progress of Plant Medicine Derived Extracts and Alkaloids on Modulating Viral Infections and Inflammation. *Drug design, development and therapy* **2021,** 15, 1385-1408.

13. Oderinlo, O. O.; Adenekan, O. A.; Alawode, T. T.; Osamudiamen, P. M.; Oluremi, B. B.; Oyeneyin, O. E.; Ngoepe, M. P., Ethnobotanical Appraisal and In-silico Investigation of Plants Used for the Management of COVID-19 in Southwestern Nigeria. *2021* **2021,** 7, (1), 24.

14. Yin, X.; Chávez León, M. A. S. C.; Osae, R.; Linus, L. O.; Qi, L.-W.; Alolga, R. N., Xylopia aethiopica Seeds from Two Countries in West Africa Exhibit Differences in Their Proteomes, Mineral Content and Bioactive Phytochemical Composition. *Molecules (Basel, Switzerland)* **2019,** 24, (10), 1979.

15. Oluremi, B.; Adeniji, J., Anti-Viral Activity Evaluation of Selected Medicinal Plants of Nigeria Against Measles Virus. *Microbiology Research Journal International* **2015,** 7, 218-225.

16. Tamfu, A. N.; Ceylan, O.; Kucukaydin, S.; Ozturk, M.; Duru, M. E.; Dinica, R. M., Antibiofilm and Enzyme Inhibitory Potentials of Two Annonaceous Food Spices, African Pepper (Xylopia aethiopica) and African Nutmeg (Monodora myristica). *Foods* **2020,** 9, (12), 1768.

17. Kumar, M.; Singh, S. K.; Singh, P. P.; Singh, V. K.; Rai, A. C.; Srivastava, A. K.; Shukla, L.; Kesawat, M. S.; Kumar Jaiswal, A.; Chung, S.-M.; Kumar, A., Potential Anti-Mycobacterium tuberculosis Activity of Plant Secondary Metabolites: Insight with Molecular Docking Interactions. *Antioxidants* **2021,** 10, (12), 1990.

18. Oyeneyin, O.; Adejoro, I. A.; Obadawo, B.; Amoko, J.; Olumide, I.; Akintemi, E.; Ipinloju, N., Investigation into the Molecular Properties of 3-(4-Hydroxyphenyl) Prop- 2-en-1-one 4-Phenyl Schiff Base and Some of Its Derivatives-DFT and Molecular Docking Studies. *Science Letters* **2021,** 9, 4-11.

19. Townsend, P. A.; Grayson, M. N., Density Functional Theory in the Prediction of Mutagenicity: A Perspective. *Chemical Research in Toxicology* **2021,** 34, (2), 179-188.

20. Hassan, T., Density Functional Theory Investigation of Some Pyridine Dicarboxylic Acids Derivatives as Corrosion Inhibitors. *International Journal of Electrochemical Science* **2020**, 4274-4286.

21. Deghady, A. M.; Hussein, R. K.; Alhamzani, A. G.; Mera, A., Density Functional Theory and Molecular Docking Investigations of the Chemical and Antibacterial Activities for 1-(4-Hydroxyphenyl)-3-phenylprop-2-en-1-one. *Molecules* **2021,** 26, (12), 3631.

22. Hussein, R. K.; Elkhair, H. M., Molecular docking identification for the efficacy of some zinc complexes with chloroquine and hydroxychloroquine against main protease of COVID-19. *Journal of Molecular Structure* **2021,** 1231, 129979.

23. Sliwoski, G.; Kothiwale, S.; Meiler, J.; Lowe, E. W., Jr., Computational methods in drug discovery. *Pharmacological reviews* **2013,** 66, (1), 334-395.

24. Fetse, J. P.; Kofie, W.; Adosraku, R., Ethnopharmacological Importance of Xylopia Aethiopica (DUNAL) A. RICH (Annonaceae) - A Review. *Journal of Pharmaceutical Research International* **2016,** 11, 1-21.

25. Trott, O.; Olson, A. J., AutoDock Vina: improving the speed and accuracy of docking with a new scoring function, efficient optimization, and multithreading. *Journal of computational chemistry* **2010,** 31, (2), 455-461.

26. Daina, A.; Michielin, O.; Zoete, V., SwissADME: a free web tool to evaluate pharmacokinetics, drug-likeness and medicinal chemistry friendliness of small molecules. *Scientific Reports* **2017,** 7, (1), 42717.

27. Verdonk, M. L.; Cole, J. C.; Hartshorn, M. J.; Murray, C. W.; Taylor, R. D., Improved protein–ligand docking using GOLD. *Proteins: Structure, Function, and Bioinformatics* **2003,** 52, (4), 609-623.

28. Bouachrine, M.; Hamidi, M.; Bouzzinea, S. M.; Taoufik, H., Theoretical study on the structure and electronic properties of new materials based on thiophene and oxadiazole. *Journal of Applied Chemical Research* **2009,** 10, (2), -.

29. Semire, B.; Oyebamiji, A. K.; Ahmad, M. S., Theoretical Study on Structure and Electronic Properties of 2, 5-Bis [4-N, N-Diethylaminostyryl] Thiophene and Its Furan and Pyrrole Derivatives Using Density Functional Theory (Dft). *Pakistan Journal of Chemistry* **2012,** 2, 166-173.

30. Arnott, J. A.; Planey, S. L., The influence of lipophilicity in drug discovery and design. *Expert opinion on drug discovery* **2012,** 7, (10), 863-875.

31. Johnson, T. W.; Gallego, R. A.; Edwards, M. P., Lipophilic Efficiency as an Important Metric in Drug Design. *Journal of Medicinal Chemistry* **2018,** 61, (15), 6401-6420.

32. Wang, J.; Skolnik, S., Recent Advances in Physicochemical and ADMET Profiling in Drug Discovery. *Chemistry & Biodiversity* **2009,** 6, (11), 1887-1899.

33. Leeson, P. D.; Springthorpe, B., The influence of drug-like concepts on decision-making in medicinal chemistry. *Nature Reviews Drug Discovery* **2007,** 6, (11), 881-890.

34. Arnott, J.; Kumar, R.; Lobo, S., Lipophilicity Indices for Drug Development. *Journal of Applied Biopharmaceutics and Pharmacokinetics* **2013,** 1, 31-36.

35. Meanwell, N. A., Synopsis of Some Recent Tactical Application of Bioisosteres in Drug Design. *Journal of Medicinal Chemistry* **2011,** 54, (8), 2529-2591.

36. Oyewole, R. O.; Oyebamiji, A. K.; Semire, B., Theoretical calculations of molecular descriptors for anticancer activities of 1, 2, 3-triazole-pyrimidine derivatives against gastric cancer cell line (MGC-803): DFT, QSAR and docking approaches. *Heliyon* **2020,** 6, (5), e03926.

37. Debenedetti, P., Condensed matter. *J of Phy* **2003,** 15, 1669.

38. Lewis, D. F. V.; Broughton, H. B., Molecular Binding Interactions: Their Estimation and Rationalization in QSARs in Terms of Theoretically Derived Parameters. *The Scientific World Journal* **2002,** 2, 202353.

39. Gupta, M.; Sharma, R.; Kumar, A., Docking techniques in pharmacology: How much promising? *Computational Biology and Chemistry* **2018,** 76, 210-217.

40. Mpiana, P. T.; Ngbolua, K.-t.-N.; Tshibangu, D. S. T.; Kilembe, J. T.; Gbolo, B. Z.; Mwanangombo, D. T.; Inkoto, C. L.; Lengbiye, E. M.; Mbadiko, C. M.; Matondo, A.; Bongo, G. N.; Tshilanda, D. D., Identification of potential inhibitors of SARS-CoV-2 main protease from Aloe vera compounds: A molecular docking study. *Chemical Physics Letters* **2020,** 754, 137751.

41. Alfaro, M.; Alfaro, I.; Angel, C., Identification of potential inhibitors of SARS-CoV-2 papain-like protease from tropane alkaloids from Schizanthus porrigens: A molecular docking study. *Chemical Physics Letters* **2020,** 761, 138068.

42. Enmozhi, S. K.; Raja, K.; Sebastine, I.; Joseph, J., Andrographolide as a potential inhibitor of SARS-CoV-2 main protease: an in silico approach. *Journal of biomolecular structure & dynamics* **2021,** 39, (9), 3092-3098.

43. Veber, D. F.; Johnson, S. R.; Cheng, H.-Y.; Smith, B. R.; Ward, K. W.; Kopple, K. D., Molecular Properties That Influence the Oral Bioavailability of Drug Candidates. *Journal of Medicinal Chemistry* **2002,** 45, (12), 2615-2623.

44. Muegge, I., Selection criteria for drug-like compounds. *Medicinal Research Reviews* **2003,** 23, (3), 302-321.

45. Lipinski, C. A.; Lombardo, F.; Dominy, B. W.; Feeney, P. J., Experimental and computational approaches to estimate solubility and permeability in drug discovery and development settings. *Advanced Drug Delivery Reviews* **1997,** 23, (1), 3-25.

46. Blake, J. F., Chemoinformatics – predicting the physicochemical properties of 'drug-like' molecules. *Current Opinion in Biotechnology* **2000,** 11, (1), 104-107.

47. Chico, L. K.; Van Eldik, L. J.; Watterson, D. M., Targeting protein kinases in central nervous system disorders. *Nature Reviews Drug Discovery* **2009,** 8, (11), 892-909.

.